Uplink Interference Analysis for Two-tier Cellular Networks with Diverse Users under Random Spatial Patterns

Wei Bao and Ben Liang
Department of Electrical and Computer Engineering, University of Toronto
Email: {wbao, liang}@comm.utoronto.ca

***Abstract*—Multi-tier architecture improves the spatial reuse of radio spectrum in cellular networks, and user classification allows consideration for diverse user service requirements. But they introduce complicated heterogeneity in the spatial distribution of transmitters, which brings to new challenges in interference analysis. In this work, we present a stochastic geometric model to evaluate the uplink interference in a two-tier network considering multi-type tier-1 users, tier-2 cells and tier-2 users. Each type of tier-1 users and tier-2 base stations are modeled as independent homogeneous Poisson point process, and each type of tier-2 users are modeled as local non-homogeneous Poisson point process centered at tier-2 base stations. By applying a superposition-aggregation-superposition (SAS) approach, we numerically characterize the interference at of both tiers. Finally, simulation results validate our model and illustrate that our model offers substantial improvement in accuracy compared with the best known approximation model.**

I. Introduction

In designing wireless celluar networks, one aim is to provide higher capacity, better quality, lower power usage, and ubiquitous coverage. To achieve this goal, one efficient way is to install a second tier of smaller cells, such as distributed antennas, relays, and femtocells, overlaying the original tier-1 cells. Each tier-2 cell is centered at a base station with shorter-range and lower-cost, which is connected to the core network through cable or digital subscriber line. By doing so, the tier-2 network could provide nearby users with higher-quality and lower-power usage communication links.

However, with such tier-2 facilities, interference management becomes more challenging. *First*, the spatial patterns of different network components vary significantly, leading to a more complicated interference environment. Tier-1 BSs are designed and deployed regularly by the network operator; tier-1 users are randomly distributed in the system; tier-2 BSs are deployed irregularly, sometimes in an "anywhere plug and play" manner (e.g., femtocell BSs), implying a high level of spatial randomness; the distribution of tier-2 users are even more complicated: they are not only randomly distributed, but also show spatial correlations, because they are likely to aggregate around tier-2 BSs. Because each network component contributes to the total interference differently, their overall effect is difficult to characterize. *Second*, multiple types of user equipments (UEs) are included in the network, where each type is distinguished by the requirement of transmission quality (e.g., transmission power and targeted SINR). Tier-2 cells may also be classified into different types according to their communication range (e.g., microcell, picocell, and femtocell) and their local load. Such diverse UEs and tier-2 cells introduce more challenges in the interference analysis.

This work has been supported in part by grants from Bell Canada and the Natural Sciences and Engineering Research Council (NSERC) of Canada.

Stochastic geometry is a promising mathematical tool to analyze the interference of cellular networks [1]. Interferers can be modeled as a Poisson point process (PPP), and their interference can be analyzed as the shot noise [2], [3] on the two dimensional Euclidean space. The Laplace transform of the shot noise can be derived directly from the Laplace functional [2], [3] or the generating functional [4] of the PPP. In this way, the interference can be analyzed mathematically. System metrics, such as outage probability and system throughput can then be deducted from the Laplace transform of the interference.

By employing the stochastic geometry approach, the downlink interference of multi-tier cellular networks was well studied in [5]–[7], and the uplink interference of single tier cellular network was studied in [8]–[10]. However, to analyze the *uplink interference in two-tier networks* is more challenging, as we need to account for the spatial randomness and correlation of tier-2 UEs aggregating around tier-2 BSs. Innovative efforts have been made in previous works, but they only partially solve the challenges. Without using stochastic geometry, [11] studied the uplink performance of a single tier-1 cell and a single tier-2 cell, while [12] extended it to the case of multiple tier-1 cells and multiple tier-2 cells. However, their model was based on a fixed number of tier-1 and tier-2 cells, without considering the random spatial patterns of UEs and BSs. [13] evaluated the uplink performance of two-tier networks with random spatial patterns with a single type of UEs and tier-2 cells. Several interference components were analyzed based on approximations: 1) The inter-interference of tier-1 cell is estimated as truncated Gaussian distributed; 2) The radius of tier-2 cells are regarded as zero when viewed from the outside; 3) Tier-2 UEs are assumed to transmit at the maximum power at the edge of tier-2 cells; 4) The cross interference from tier-1 UEs to tier-2 BSs only accounts for the interference from a reference tier-1 cell. [14] studied both uplink and downlink interference of two-tier network based on a Neyman-Scott Process [4], [15]. However [14] is also limited in two aspects: 1) Each UE is assumed to transmit at the same power; 2) Tier-2 users are assumed to be uniformly distributed in an infinitesimally thin ring around the tier-2 BS. In addition, neither [13] nor [14] considered multi-type UEs or tier-2 cells.

In this work, we propose an accurate uplink interference model of two-tier cellular networks, considering multiple types of tier-1 UEs, tier-2 BSs, and tier-2 UEs. At tier-1, the interference is studied as the shot noise corresponding to PPPs. At tier-2, we develop a *superposition-aggregation-superposition (SAS)* approach to overcome the challenges in analysis. *First*,

within each tier-2 cell, the overall interference by UEs is the superposition over multiple types of UEs; second, the interference from each tier-2 cell is equivalently aggregated as a single point interference source at the corresponding tier-2 BS; third, the overall interference by tier-2 cells is again the superposition over multiple types of tier-2 cells. Through this SAS approach, we precisely compute the interference of both tiers, avoiding any approximations. To the best of our knowledge, this paper is the first work to accurately analyze the uplink interference of two-tier network with diverse users under random spatial patterns.

The rest of the paper is organized as follows. In Section II, we present the system model. In Section III and IV, we analyze the interference of tier-1 cells and tier-2 cells, respectively. In Section V, we validate our model with simulation results. Finally, concluding remarks are given in Section VI.

II. System Model

A. System Structure

In this subsection, we present the system structure considered in this work, which is shown in Fig. 1. First, because the tier-1 BSs are designed and deployed by the network operator in a more regulated manner, following the convention in literature, we assume that the tier-1 cells form an infinite hexagonal grid on the two-dimensional Euclidean space $\mathbb{R}^2$. Tier-1 BSs are located at the centers of the hexagons $\mathbb{B} = \{(\frac{3}{2}aR_c, \frac{\sqrt{3}}{2}aR_c + \sqrt{3}bR_c) | a, b \in \mathbb{Z}\}$, where R_c is the radius of the hexagon. Tier-1 UEs are randomly distributed in the system, which are modeled as PPPs. Considering the diverse users, we assume that there are M types of tier-1 UEs. Each type independently forms a homogeneous PPP. Let Φ_i denote the PPP corresponding to type i tier-1 UEs. Its intensity is λ_i.

We also assume that there are N types of tier-2 BSs and K types of tier-2 UEs. Because tier-2 BSs are operated with high spatial randomness, we assume each type of tier-2 BSs form a homogeneous PPP. Let Θ_i denote the PPP corresponding to type i tier-2 BS. Its intensity is μ_i. Each tier-2 BS is connecting to the core network via wired network, which has no influence on the interference analysis.

Each tier-2 BS is communicating with different types of local tier-2 UEs surrounding it, composing a tier-2 cell. Let R_i $(1 \leq i \leq N)$ be the communication radius of each type i tier-2 BS, with its corresponding tier-2 UEs located within R_i from it. Given the location of a type i tier-2 BS at $\mathbf{x}_0$, we assume that each type of local tier-2 UEs are independently distributed as a non-homogenous PPP in the disk centered at $\mathbf{x}_0$ with radius R_i. Let $\Psi_{i,j}(\mathbf{x}_0)$ denote the PPP of type j $(1 \leq j \leq N)$ tier-2 UEs around a type i tier-2 BS at $\mathbf{x}_0$. Its intensity at $\mathbf{x}$ is described by $\nu_{i,j}(\mathbf{x} - \mathbf{x}_0)$, an arbitrary non-negative function of the *vector* $\mathbf{x} - \mathbf{x}_0$.[1] Note that the user intensity $\nu_{i,j}(\mathbf{x} - \mathbf{x}_0) = 0$ if $|\mathbf{x} - \mathbf{x}_0| > R_i$. We assume the tier-2 UEs in one tier-2 cell are also independent with tier-2 UEs in other tier-2 cells as well as tier-1 UEs. To better understand the distribution of tier-2 BSs and tier-2 UEs, Θ_i can be regarded as a parent point process on the plane, while $\Psi_{i,j}$ is a daughter processes associated with a point in the parent point process. Note that the aggregating of tier-2 UEs around a tier-2 BS implicitly defines the location correlation among tier-2 UEs. Since there is a one-to-one mapping between tier-2 cells and tier-2 BSs, we will view the two terms interchangeably.

[1] Our model is more general compared with the assumptions in [13] and [14] by allowing inhomogeneity in tier-2 cells.

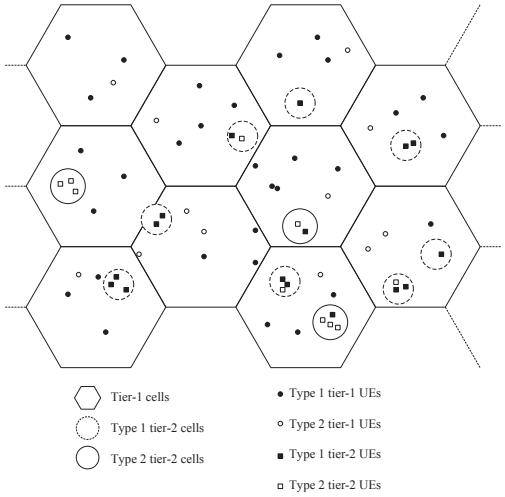

Fig. 1. System model.

Because we focus on the uplink interference analysis, we assume that the downlink and uplink of the system are operated in different spectrum, thus the downlink interference has no influence on the interference analysis in this paper.

Let $\mathcal{H}(\mathbf{x})$ denote the hexagon region centered at $\mathbf{x}$ with radius R_c; let $\mathcal{B}(\mathbf{x}, R)$ denote the disk region centered at $\mathbf{x}$ with radius R.

B. Pathloss Model and Power Control

Let $P_t(\mathbf{x})$ denote the transmission power at $\mathbf{x}$ and $P_r(\mathbf{y})$ denote the received power at $\mathbf{y}$. We assume that $P_r(\mathbf{y}) = \frac{P_t(\mathbf{x}) g_{\mathbf{x}} g_{\mathbf{x},\mathbf{y}} h_{\mathbf{x},\mathbf{y}}}{A|\mathbf{x}-\mathbf{y}|^\gamma}$, where $A|\mathbf{x} - \mathbf{y}|^\gamma$ is the propagation loss function with predetermined constants A and γ, $g_{\mathbf{x}} g_{\mathbf{x},\mathbf{y}}$ is the shadowing term, which is composed of the near field factor $g_{\mathbf{x}}$ and far field factor $g_{\mathbf{x},\mathbf{y}}$ [16], and $h_{\mathbf{x},\mathbf{y}}$ is the fast fading term. Here, $g_{\mathbf{x}}$ and $g_{\mathbf{x},\mathbf{y}}$ are independently log-normal distributed with given parameters, and $h_{\mathbf{x},\mathbf{y}}$ is independently exponentially distributed with unit mean (Rayleigh fading with power normalization).

We follow the conventional assumption that uplink power control adjusts for propagation losses and shadowing [8], [13], [16], [17]. The targeted power level for type i tier-1 UEs is P_i, and the targeted power for type j tier-2 UEs in type i tier-2 cells is $Q_{i,j}$. Given the targeted received power P (i.e., $P = P_i$ or $P = Q_{i,j}$) at $\mathbf{y}$ and transmitter at $\mathbf{x}$, the transmission power is $\frac{PA|\mathbf{x}-\mathbf{y}|^\gamma}{g_{\mathbf{x}} g_{\mathbf{x},\mathbf{y}}}$. Then, the resultant contribution to interference at $\mathbf{y}' \neq \mathbf{y}$ is $\frac{P|\mathbf{x}-\mathbf{y}|^\gamma g_{\mathbf{x},\mathbf{y}'} h_{\mathbf{x},\mathbf{y}'}}{|\mathbf{x}-\mathbf{y}'|^\gamma g_{\mathbf{x},\mathbf{y}}}$.

Note that $g_{\mathbf{x},\mathbf{y}'}/g_{\mathbf{x},\mathbf{y}}$ is still log-normally distributed and is i.i.d. with respect to different $\mathbf{x}$, and $h_{\mathbf{x},\mathbf{y}}$ is i.i.d. with respect to different $\mathbf{x}$ and $\mathbf{y}$. Let $G(\cdot)$ be the CDF of $g_{\mathbf{x},\mathbf{y}'}/g_{\mathbf{x},\mathbf{y}}$ (log-normal), and $H(\cdot)$ be the CDF of $h_{\mathbf{x},\mathbf{y}}$ (exponential with unit mean).

C. Scope of this work

Our model is valid for both the orthogonal multiplexing case (e.g., OFDMA) and non-orthogonal multiplexing case (e.g., CDMA) [6]. For OFDMA, the spectrum is partitioned into n orthogonal resource blocks, and thus the density of UEs is equivalently reduced by a factor of n when we assume random access of each resource block. For CDMA, a spreading code is applied to transmit the signals. At a receiver, the SINR is equivalent to having a multiple of m, where m is the spreading factor.

III. Interference to Tier-1 BSs

In this section, we analyze the uplink interference at tier-1 BSs. Given a reference type k tier-1 UE, termed the *typical tier-1 UE*, communicating with its BS, termed the *typical tier-1 BS*, we compute the interference of all other tier-1 and tier-2 UEs at the typical BS. Due to stationarity of point processes corresponding to tier-1 UEs, tier-2 BSs, and tier-2 UEs, throughout this section we will re-define the coordinates so that the typical UE is located at $\mathbf{0}$[2]. Since tier-1 BSs form a deterministic hexagonal grid, the typical BS is then uniformly distributed in $\mathcal{H}(\mathbf{0})$ [2]. Let Φ_k' denote the point process of all other type k tier-1 UEs conditioned on the typical UE at $\mathbf{0}$ (i.e., the reduced Palm point process with respect to Φ_k). Since the reduced Palm point process of a PPP has the same distribution as the original PPP, Φ_k' is still a PPP with intensity λ_k [2]. For presentation convenience, we define $\widetilde{\Phi}_i$, such that $\widetilde{\Phi}_i = \Phi_i$ if $i \neq k$ and $\widetilde{\Phi}_i = \Phi_i'$ if $i = k$. Note that the above typicality definition and the coordination translation follow standard stochastic geometric techniques.

In the following work, instead of directly computing the distribution of interference, we study its Laplace transform (i.e., moment generating function), which fully characterizes its distribution.

A. Interference from Tier-1 UEs to Tier-1 BS

First, we compute the Laplace transform of the interference produced by tier-1 UEs, to the typical tier-1 BS located at $\mathbf{x}_B$.

Let $I_{1,in,i}(\mathbf{x}_B)$ denote the total interference from type i tier-1 UEs inside the typical cell $\mathcal{H}(\mathbf{x}_B)$, and $I_{1,out,i}(\mathbf{x}_B)$ denote the total interference from type i tier-1 UEs outside the typical cell. We have

$$I_{1,in,i}(\mathbf{x}_B) = \sum_{\mathbf{x}\in\widetilde{\Phi}_i \bigcap \mathcal{H}(\mathbf{x}_B)} P_i h_{\mathbf{x},\mathbf{x}_B}, \tag{1}$$

$$I_{1,out,i}(\mathbf{x}_B) = \sum_{\substack{\mathbf{x}_0\in \\ \mathbb{B}-\mathbf{x}_B\setminus\{\mathbf{0}\}}} \sum_{\substack{\mathbf{x}\in\widetilde{\Phi}_i\bigcap \\ \mathcal{H}(\mathbf{x}_0)}} \frac{P_i|\mathbf{x}-\mathbf{x}_0|^\gamma g_{\mathbf{x}+\mathbf{x}_B,\mathbf{x}_B} h_{\mathbf{x}+\mathbf{x}_B,\mathbf{x}_B}}{|\mathbf{x}|^\gamma g_{\mathbf{x}+\mathbf{x}_B,\mathbf{x}_0+\mathbf{x}_B}}. \tag{2}$$

$I_{1,in,i}(\mathbf{x}_B)$ and $I_{1,out,i}(\mathbf{x}_B)$ can be regarded as shot noises corresponding to $\widetilde{\Phi}_i$. The sum form of (1) and (2) is converted to the product form in Laplace transform, which can then be matched to the form of Laplace functionals corresponding to the PPP [2]. Thus, we have

$$\mathcal{L}_{I_{1,in,i}(\mathbf{x}_B)}(s) = \mathbf{E}(e^{-sI_{1,in,i}(\mathbf{x}_B)}) = \exp\left(-\lambda_i(3\sqrt{3}/2)R_c^2\left(1-\int_{\mathbb{R}^+} e^{-sP_i h}H(dh)\right)\right), \tag{3}$$

$$\mathcal{L}_{I_{1,out,i}(\mathbf{x}_B)}(s) = \exp\left(-\lambda_i \sum_{\mathbf{x}_0\in\mathbb{B}-\mathbf{x}_B\setminus\{\mathbf{0}\}} \int_{\mathcal{H}(\mathbf{x}_0)} \left(1- \int_{\mathbb{R}^+}\int_{\mathbb{R}^+} e^{-\frac{sP_i|\mathbf{x}-\mathbf{x}_0|^\gamma gh}{|\mathbf{x}|^\gamma}} G(dg)H(dh)\right)d\mathbf{x}\right). \tag{4}$$

Note that $\mathcal{L}_{I_{1,in,i}(\mathbf{x}_B)}(s)$ and $\mathcal{L}_{I_{1,out,i}(\mathbf{x}_B)}(s)$ do not depend on $\mathbf{x}_B$, so they can be replaced by $\mathcal{L}_{I_{1,in,i}}(s)$ and $\mathcal{L}_{I_{1,out,i}}(s)$ respectively. Due to the independence between $I_{1,in,i}(\mathbf{x}_B)$ and $I_{1,out,i}(\mathbf{x}_B)$, the Laplace transform of the overall interference from all type i tier-1 UEs to the typical tier-1 BS can be computed as

$$\mathcal{L}_{I_{1,i}}(s) = \mathcal{L}_{I_{1,in,i}}(s)\mathcal{L}_{I_{1,out,i}}(s). \tag{5}$$

Due to the independence among different types of tier-1 UEs, the Laplace transform of the overall interference from all tier-1 UEs to the typical tier-1 BS can be computed as

$$\mathcal{L}_{I_1}(s) = \prod_{i=1}^{M} \mathcal{L}_{I_{1,i}}(s). \tag{6}$$

B. Interference from Tier-2 UEs to Tier-1 BS

In this subsection, we study the interference from tier-2 UEs to the typical tier-1 BS, which is the core analysis in this work. Because all the tier-2 UEs are correlated distributed around tier-2 BSs, it cannot be analyzed by a traditional stochastic geometric approach. Instead, we propose the *superposition-aggregation-superposition* approach, which perfectly captures the interference from tier-2 cells.

Interference from One Tier-2 Cell: In the first step, we study the interference from a single type of tier-2 UEs in a single tier-2 cell. Let $\widehat{I}_{2,i}(\mathbf{x}_0,\mathbf{x}_B)$ be the interference from a single type i tier-2 cell, whose BS is at $\mathbf{x}_0$, to the typical tier-1 BS located at $\mathbf{x}_B$. $\widehat{I}_{2,i}(\mathbf{x}_0,\mathbf{x}_B) = \sum_{j=1}^{K}\widehat{I}_{2,i,j}(\mathbf{x}_0,\mathbf{x}_B)$, where $\widehat{I}_{2,i,j}$ is the interference from all type j tier-2 UEs in the single type i tier-2 cell. We have

$$\widehat{I}_{2,i,j}(\mathbf{x}_0,\mathbf{x}_B) = \sum_{\mathbf{x}\in\Psi_{i,j}(\mathbf{x}_0)} \frac{Q_{i,j}|\mathbf{x}-\mathbf{x}_0|^\gamma g_{\mathbf{x},\mathbf{x}_B} h_{\mathbf{x},\mathbf{x}_B}}{|\mathbf{x}-\mathbf{x}_B|^\gamma g_{\mathbf{x},\mathbf{x}_0}}. \tag{7}$$

Its Laplace transform can be derived through the Laplace functional corresponding to $\Psi_{i,j}(\mathbf{x}_0)$,

$$\mathcal{L}_{\widehat{I}_{2,i,j}(\mathbf{x}_0,\mathbf{x}_B)}(s) = \exp\left(-\int_{\mathcal{B}(\mathbf{0},R_i)} \left(1- \int_{\mathbb{R}^+}\int_{\mathbb{R}^+} e^{-\frac{sQ_{i,j}|\mathbf{x}|^\gamma gh}{|\mathbf{x}+\mathbf{x}_0-\mathbf{x}_B|^\gamma}} H(dh)G(dg)\right)\nu_{i,j}(\mathbf{x})d\mathbf{x}\right). \tag{8}$$

Because the entire set of tier-2 UEs associated with the tier-2 BS located at $\mathbf{x}_0$ can be regarded as a *independent*

[2]Given the coordinate of the typical tier-1 BS $\mathbf{x}_B$, the coordinates of all tier-1 BSs are redefined as $\mathbb{B} = \{(\frac{3}{2}aR_c, \frac{\sqrt{3}}{2}aR_c+\sqrt{3}bR_c)+\mathbf{x}_B|a,b\in\mathbb{Z}\}$.

superposition of multiple types of tier-2 UEs, the Laplace transform of $\widehat{I}_{2,i}(\mathbf{x}_0, \mathbf{x}_B)$ can be computed as

$$\mathcal{L}_{\widehat{I}_{2,i}(\mathbf{x}_0,\mathbf{x}_B)}(s) = \prod_{j=1}^{K} \mathcal{L}_{\widehat{I}_{2,i,j}(\mathbf{x}_0,\mathbf{x}_B)}(s). \tag{9}$$

Note that $\mathcal{L}_{\widehat{I}_{2,i,j}(\mathbf{x}_0,\mathbf{x}_B)}(s)$ and $\mathcal{L}_{\widehat{I}_{2,i}(\mathbf{x}_0,\mathbf{x}_B)}(s)$ are functions related to *a unique coordinate* $\mathbf{x}_0 - \mathbf{x}_B$, so we can replace them by $\mathcal{L}_{\widehat{I}_{2,i,j}(\mathbf{x}_0-\mathbf{x}_B)}(s)$ and $\mathcal{L}_{\widehat{I}_{2,i}(\mathbf{x}_0-\mathbf{x}_B)}(s)$ respectively. This provides a very important property in the following analysis, that the interference from one cell can be equivalently regarded as emission from one *aggregation* point at $\mathbf{x}_0 - \mathbf{x}_B$. As a consequence, we can use a function of the aggregation point to represent the overall interference corresponding to one tier-2 cell.

Overall Interference: Based on the above conclusion, we can study the overall interference from a single type of tier-2 cells.

Let $I_{2,i}(\mathbf{x}_B)$ denote the total interference from type i tier-2 cells to the typical tier-1 BS. We have

$$I_{2,i}(\mathbf{x}_B) = \sum_{\mathbf{x}\in\Theta_i} \widehat{I}_{2,i}(\mathbf{x}, \mathbf{x}_B). \tag{10}$$

Thus, we can derive the Laplace transform of $I_{2,i}(\mathbf{x}_B)$ as follows:

$$\begin{aligned}
\mathcal{L}_{I_{2,i}(\mathbf{x}_B)}(s) &= \mathbf{E}\left(\prod_{\mathbf{x}\in\Theta_i} e^{-s\widehat{I}_{2,i}(\mathbf{x},\mathbf{x}_B)}\right) \\
&= \mathbf{E}\left(\prod_{\mathbf{x}\in\Theta_i} \mathbf{E}\left(e^{-s\widehat{I}_{2,i}(\mathbf{x},\mathbf{x}_B)}|\Theta_i\right)\right) && (11)\\
&= \mathbf{E}\left(\prod_{\mathbf{x}\in\Theta_i} \mathcal{L}_{\widehat{I}_{2,i}(\mathbf{x}-\mathbf{x}_B)}(s)\right) && (12)\\
&= \exp\left(-\mu_i \int_{\mathbb{R}^2} (1 - \mathcal{L}_{\widehat{I}_{2,i}(\mathbf{x}-\mathbf{x}_B)}(s)) d\mathbf{x}\right) && (13)\\
&= \exp\left(-\mu_i \int_{\mathbb{R}^2} (1 - \mathcal{L}_{\widehat{I}_{2,i}(\mathbf{x})}(s)) d\mathbf{x}\right), && (14)
\end{aligned}$$

in which we substitute (9) into (11) to derive (12), where the interference $\widehat{I}_{2,i}(\mathbf{x}, \mathbf{x}_B)$ can be replaced by the function of the aggregation point $\mathbf{x} - \mathbf{x}_B$. As a consequence, the item $\mathbf{E}\left(\prod_{\mathbf{x}\in\Theta_i} \mathcal{L}_{\widehat{I}_{2,i}(\mathbf{x}-\mathbf{x}_B)}(s)\right)$ in (12) is in the exactly the same form as the generating functional of the PPP Θ_i, which can then be converted to the integral form in (13) [4]. Note that $\mathcal{L}_{I_{2,i}(\mathbf{x}_B)}(s)$ does not depend on $\mathbf{x}_B$, so it can be replaced by $\mathcal{L}_{I_{2,i}}(s)$.

Let I_2 denote the total interference from tier-2 UEs to the typical tier-1 BS. Because multi-type tier-2 BSs can be regarded as *independent superposition* of each type of tier-2 BSs, the Laplace transform $\mathcal{L}_{I_2}$ can be computed as

$$\mathcal{L}_{I_2}(s) = \prod_{i=1}^{N} \mathcal{L}_{I_{2,i}}(s). \tag{15}$$

C. Overall Interference and Outage at Tier-1 Cell

Since tier-1 UEs and tier-2 UEs are independent, the Laplace transform of the total interference is

$$\mathcal{L}_I(s) = \mathcal{L}_{I_1}(s)\mathcal{L}_{I_2}(s). \tag{16}$$

Note that the statistics of the interference is irrelevant to k, the type of the typical tier-1 UEs communicating with the typical BS.

Then, given an SINR threshold T, the outage probability for the type k tier-1 UE is given by

$$\begin{aligned}
P_{out,k} &= \mathbf{P}(P_k h_{\mathbf{0},\mathbf{x}_B} < T(I + W)) \\
&= 1 - \mathcal{L}_I(T/P_k)\mathcal{L}_W(T/P_k). && (17)
\end{aligned}$$

where random variable W denotes the power of thermal noise and $L_W(\cdot)$ is its Laplace transform, and (17) is due to $h_{\mathbf{0},\mathbf{x}_B}$ being exponentially distributed with unit mean.

IV. Interference to Tier-2 BSs

In this section, we analyze the uplink interference at a reference type l tier-2 BS, termed the *typical tier-2 BS*, when it is communicating with a reference type k tier-2 UE termed the *typical tier-2 UE*. The *typical tier-1 BS* in this section is defined as the tier-1 BS nearest to the typical tier-2 BS. Throughout this section we will re-define the coordinates so that the typical tier-2 BS is located at $\mathbf{0}$. (Note that the coordinates in Sections III and IV are re-defined and hence labeled differently.)

A. Interference from Tier-1 UEs to Tier-2 BS

Given the typical tier-2 BS at $\mathbf{0}$, the typical tier-1 BS is uniformly distributed in $\mathcal{H}(\mathbf{0})$. If it is at $\mathbf{x}_B$, the interference from type i tier-1 UEs to the typical tier-2 BS is

$$I'_{1,i}(\mathbf{x}_B) = \sum_{\mathbf{x}_0\in\mathbb{B}} \sum_{\mathbf{x}\in\Phi_i \bigcap \mathcal{H}(\mathbf{x}_0)} \frac{P_i |\mathbf{x} - \mathbf{x}_0|^\gamma g_{\mathbf{x},\mathbf{0}} h_{\mathbf{x},\mathbf{0}}}{|\mathbf{x}|^\gamma g_{\mathbf{x},\mathbf{x}_0}},$$

with Laplace transform

$$\begin{aligned}
\mathcal{L}_{I'_{1,i}(\mathbf{x}_B)}(s) = \exp\Bigg(-\lambda_i \sum_{\mathbf{x}_0\in\mathbb{B}} \int_{\mathcal{H}(\mathbf{x}_0)} \Bigg(1 - \\
\int_{\mathbb{R}^+}\int_{\mathbb{R}^+} e^{-\frac{sP_i|\mathbf{x}-\mathbf{x}_0|^\gamma gh}{|\mathbf{x}|^\gamma}} G(dg)H(dh)\Bigg) d\mathbf{x}\Bigg). \qquad (18)
\end{aligned}$$

Due to the independence of different types of UEs, the Laplace transform of the interference from all tier-1 UEs is

$$\mathcal{L}_{I'_1(\mathbf{x}_B)}(s) = \prod_{i=1}^{M} \mathcal{L}_{I'_{1,i}(\mathbf{x}_B)}(s). \tag{19}$$

B. Inter-Cell Interference from Tier-2 UEs to Tier-2 BS

Conditioned on the typical tier-2 BS at $\mathbf{0}$, let Θ'_l denote the reduced Palm point process of the other type l tier-2 BSs. Then Θ'_l has the same distribution as Θ_l [2]. This also implies that the overall tier-2 user distribution conditioned on the typical tier-2 BS is exactly the same with the overall user distribution conditioned on the typical tier-1 UE as we discussed in Section III. Thus, the overall interference to the typical tier-2 BS has the same distribution as the interference to the typical tier-1 BS:

$$\mathcal{L}_{I'_2}(s) = \mathcal{L}_{I_2}(s). \tag{20}$$

C. Intra-Cell Interference from Tier-2 UEs to Tier-2 BS

In this subsection, we consider the interference within the typical tier-2 cell, given that the typical type k tier-2 UE is located at $\mathbf{y}_0$, $\mathbf{y}_0 \in \mathcal{B}(\mathbf{0}, R_l)$. Let $\Psi'_{l,k}(\mathbf{0})$ denote the reduced Palm point process of the other type k tier-2 UEs in the typical tier-2 cell. Then $\Psi'_{l,k}(\mathbf{0})$ has the same distribution as $\Psi_{l,k}(\mathbf{0})$. For presentation convenience, we define $\widetilde{\Psi}_{l,j}(\mathbf{0})$, such that $\widetilde{\Psi}_{l,j}(\mathbf{0}) = \Psi_{l,j}(\mathbf{0})$ if $k \neq j$ and $\widetilde{\Psi}_{l,j}(\mathbf{0}) = \Psi'_{l,j}(\mathbf{0})$ if $k = j$.

The intra-cell interference of the type j tier-2 UEs is

$$I'_{3,j}(\mathbf{x}_B, \mathbf{y}_0) = \sum_{\mathbf{x} \in \widetilde{\Psi}_{l,j}(\mathbf{0})} Q_{l,j} h_{\mathbf{x},\mathbf{0}}, \tag{21}$$

with Laplace transform

$$\mathcal{L}_{I'_{3,j}(\mathbf{x}_B,\mathbf{y}_0)}(s) = \exp\left(- \int_{\mathcal{B}(\mathbf{0},R_l)} \left(1 - \int_{\mathbb{R}^+} e^{-sQ_{l,j}h} H(dh) \right) \nu_{l,j}(\mathbf{x}) d\mathbf{x} \right), \tag{22}$$

which is irrelevant with $\mathbf{x}_B$ or $\mathbf{y}_0$. Thus, it can be replaced by $\mathcal{L}_{I'_{3,j}}(s)$.

The Laplace transform of overall interference inside the typical tier-2 cell is

$$\mathcal{L}_{I'_3}(s) = \prod_{j=1}^{K} \mathcal{L}_{I'_{3,j}}(s). \tag{23}$$

D. Overall Interference and Outage at Tier-2 Cell

The Laplace transform of overall interference is an average over $\mathbf{x}_B$, thus,

$$\mathcal{L}_{I'}(s) = \frac{\mathcal{L}_{I'_2}(s)\mathcal{L}_{I'_3}(s) \int_{\mathcal{H}(\mathbf{0})} \mathcal{L}_{I'_1(\mathbf{x}_B)}(s) d\mathbf{x}_B}{\left(3\sqrt{3}/2R_c^2\right)}. \tag{24}$$

Then, given an SINR threshold T, the outage probability for type k tier-2 UEs in a type l tier-2 cell is given by

$$P'_{out,l,k} = 1 - \mathcal{L}_{I'}(T/Q_{l,k})\mathcal{L}_W(T/Q_{l,k}). \tag{25}$$

V. Numerical Study

In this section, we present a numerical study of our model. Unless otherwise stated, $R_c = 1000$ m, $\gamma = 4$, the shadowing term g is log-normal with mean 0 and standard deviation 4 dB, fast fading is Rayleigh with unit mean, and the thermal noise is set to zero. Each simulation data point is averaged over 10000 trials. In the figures, the error bars show the 95% confidence intervals for simulation results.

A. Model Comparison

First, we compare our system model with the approximations made in [13]. Since [13] does not consider multi-type UEs or BSs, our comparison is based on the case where there is one type of tier-1 UEs, tier-2 cells, and tier-2 UEs (i.e., $M = N = K = 1$). In addition, since [13] ignores the effect of fast fading, instead of comparing directly with the numerical results reported there, we use a version of the proposed model, which considers fast fading but also uses the four approximating assumptions stated in Section I in the way of [13].

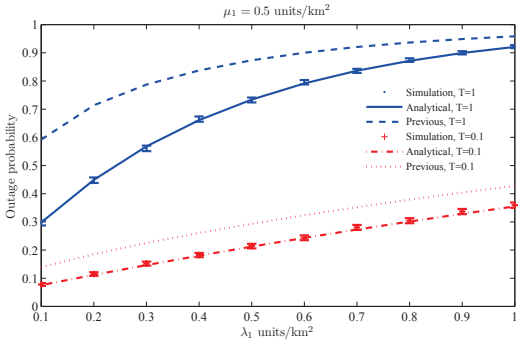

Fig. 2. Outage probability of tier-1 cells under different λ_1.

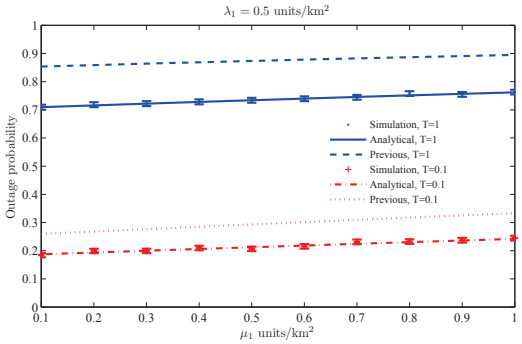

Fig. 3. Outage probability of tier-1 cells under different μ_1.

We set $R_1 = 200$ m, $\nu_{1,1}(\mathbf{x}) = 20$ units/km^2 if $|\mathbf{x}| < R_1$, $\nu_{1,1}(\mathbf{x}) = 0$ otherwise, and $P_1 = Q_{1,1} = -70$ dBm.

Fig. 2 and 3 show the uplink outage probability of tier-1 cells under different λ_1 and μ_1 respectively[3]. The figures illustrate that our analytical results are accurate and offers substantial improvement over the approximation model of [13]. In the approximation model, because tier-2 UEs are assumed to be located at the edge of tier-2 cells and transmitting with maximum power, the interference from tier-2 UEs to tier-1 BSs (as well as tier-2 BSs) is overestimated. Also, when the tier-1 inter-cell interference is approximated as truncated Gaussian, larger evaluation error occurs. Overall, the outage probabilities of tier-1 uplinks are overestimated by the approximated model.

Fig. 4 and 5 show the uplink outage probability of tier-2 cells under different λ_1 and μ_1 respectively. The figures again illustrate that our analytical results are accurate and offer substantial improvement. In the approximation model, because the interference from tier-1 UEs outside the reference tier-1 cell is ignored, the cross-tier interference from tier-1 UEs to tier-2 BSs is greatly underestimated. Even though the co-tier interference from tier-2 UEs to tier-2 BSs is overestimated, that cannot compensate for the underestimation of the cross-tier interference. Hence, overall, the outage probabilities of tier-2 uplinks are underestimated by the approximated model.

[3]As discuss in Section II-C, these intensities may already account for the multiplicative factor introduced by orthogonal multiplexing.

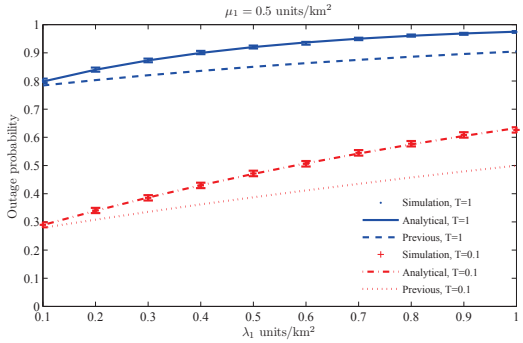

Fig. 4. Outage probability of tier-2 cells under different λ_1.

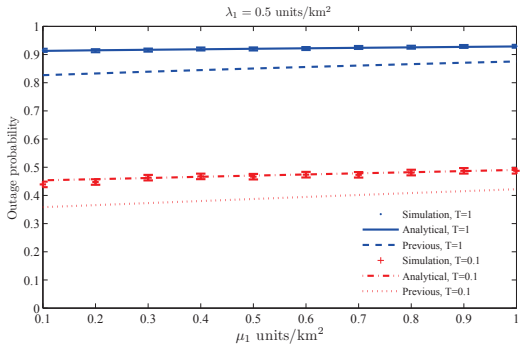

Fig. 5. Outage probability of tier-2 cells under different μ_1.

B. Outage Probability at Different Tiers

In this subsection, we study the outage probabilities of different tiers and types. The network parameters are $M = N = K = 2$, $\lambda_1 = \lambda_2 = 0.5$ units/km^2, $P_1 = -67$ dBm, $P_2 = -65.2$ dBm, $R_1 = 100$ m, $R_2 = 200$ m, $\nu_{1,1}(\mathbf{x}) = 10$ units/km^2, $\nu_{1,2}(\mathbf{x}) = 15$ units/km^2 if $|\mathbf{x}| < R_1$, $\nu_{2,1}(\mathbf{x}) = 5$ units/km^2, $\nu_{2,2}(\mathbf{x}) = 20$ units/km^2 if $|\mathbf{x}| < R_2$, $Q_{1,1} = -70$ dBm, $Q_{1,2} = -64$ dBm, $Q_{2,1} = Q_{2,2} = -67$ dBm, and $T = 0.1$.

Fig. 6 shows the analytical and simulation outage probabilities of different types and tiers. The simulation results agree with the analytical results, validating the correctness of our model. Fig. 6 also shows that at both tiers, the power P_i or $Q_{i,j}$ is a key factor to influence the outage probability. At tier-1, because $P_2 > P_1$, the outage probability of type 2 tier-1 UEs is smaller. At tier-2, $Q_{1,2} > Q_{1,1}$ leads to smaller outage probability for type 2 tier-2 UEs; while $Q_{2,2} = Q_{2,1}$ leads to the same outage probabilities. Given an arbitrary typical UE, the Palm distribution of other UEs (i.e., interferers) remains the same as their original Poisson distribution. Thus, the distribution of interference remains the same. The effect of multiple types of UEs only manifests in the shape of the common distribution of interference.

VI. Conclusions

We have proposed a stochastic geometric model to accurately quantify the uplink interference and outage performance of two-tier cellular networks with diverse users and tier-2 cells. By applying our SAS approach, we derived the numerical expressions for the Laplace transform of interference at both tiers, which avoid the approximations required in prior works, leading to accurate calculation of the outage probability. Simulations showed the validity of our model and substantial improvement in accuracy compared with the best known model [13].

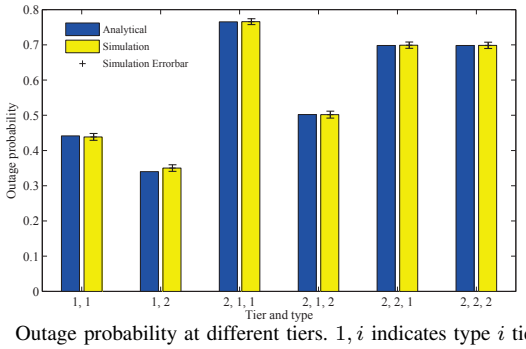

Fig. 6. Outage probability at different tiers. $1, i$ indicates type i tier-1 UEs; $2, i, j$ indicates type j tier-2 UEs in type i tier-2 cells.

References

[1] M. Haenggi, J. Andrews, F. Baccelli, O. Dousse, and M. Franceschetti, "Stochastic geometry and random graphs for the analysis and design of wireless networks," *IEEE Journal on Selected Areas in Communications*, vol. 27, no. 7, pp. 1029 – 1046, Sept. 2009.

[2] F. Baccelli and B. Blaszczyszyn, "Stochastic geometry and wireless networks, volume 1: Theory," *Foundations and Trends in Networking*, vol. 3, no. 3-4, pp. 249 – 449, 2009.

[3] ——, "Stochastic geometry and wireless networks, volume 2: Applications," *Foundations and Trends in Networking*, vol. 4, no. 1-2, pp. 1–312, 2009.

[4] D. Stoyan, W. Kendall, and J. Mecke, *Stochastic Geometry and Its Applications*, 2nd ed. Wiley, 1995.

[5] H. Dhillon, R. Ganti, F. Baccelli, and J. Andrews, "A tractable framework for coverage and outage in heterogeneous cellular networks," in *Information Theory and Applications Workshop*, San Diego, CA, Feb. 2011.

[6] ——, "Modeling and analysis of K-tier downlink heterogeneous cellular networks," *IEEE Journal on Selected Areas in Communications*, vol. 30, no. 3, pp. 550–560, Apr. 2012.

[7] Y. Kim, S. Lee, and D. Hong, "Performance analysis of two-tier femtocell networks with outage constraints," *IEEE Trans. on Wireless Communications*, vol. 9, no. 9, pp. 2695– 2700, Sept. 2010.

[8] C. C. Chan and S. Hanly, "Calculating the outage probability in a CDMA network with spatial poisson traffic," *IEEE Trans. on Vehicular Technology*, vol. 50, no. 1, pp. 183 – 204, Jan. 2001.

[9] N. Mehta, S. Singh, and A. Molisch, "An accurate model for interference from spatially distributed shadowed users in CDMA uplinks," in *Proc. of IEEE GLOBECOM*, Honolulu, HI, Dec. 2009.

[10] T. D. Novlan, H. S. Dhillon, and J. G. Andrews, "Analytical modeling of uplink cellular networks," arXiv:1203.1304 [cs.IT], 2012.

[11] S. Kishore, L. Greenstein, H. Poor, and S. Schwartz, "Uplink user capacity in a CDMA macrocell with a hotspot microcell: exact and approximate analyses," *IEEE Trans. on Wireless Communications*, vol. 2, no. 2, pp. 364–374, Mar. 2003.

[12] ——, "Uplink user capacity in a multicell CDMA system with hotspot microcells," *IEEE Trans. on Wireless Communications*, vol. 5, no. 6, pp. 1333–1342, June 2006.

[13] V. Chandrasekhar and J. Andrews, "Uplink capacity and interference avoidance for two-tier femtocell networks," *IEEE Trans. on Wireless Communications*, vol. 8, no. 7, pp. 3498–3509, Jul. 2009.

[14] W. C. Cheung, T. Q. S. Quek, and M. Kountouris, "Stochastic analysis of two-tier networks: Effect of spectrum allocation," in *Proc. of IEEE International Conference on Acoustics, Speech and Signal Processing (ICASSP)*, Prague, Czech Republic, May 2011.

[15] R. Ganti and M. Haenggi, "Interference and outage in clustered wireless ad hoc networks," *IEEE Trans. on Information Theory*, vol. 55, no. 9, pp. 4067–4086, Sept. 2009.

[16] K. Gilhousen, I. Jacobs, R. Padovani, A. Viterbi, L. Weaver, and C. Wheatley, "On the capacity of a cellular CDMA system," *IEEE Trans. on Vehicular Technology*, vol. 40, no. 2, pp. 303–312, May 1991.

[17] S. Singh, N. Mehta, A. Molisch, and A. Mukhopadhyay, "Moment-matched lognormal modeling of uplink interference with power control and cell selection," *IEEE Trans. on Wireless Communications*, vol. 9, no. 3, pp. 932–938, Mar. 2010.